

Influence of seagrass decline on the metabolic profile of sediment microbial communities

Marsej Markovski¹, Mirjana Najdek¹, Zihao Zhao², Gerhard J. Herndl^{2,3}, and Marino Korlević^{1*}

1. Centre for Marine Research, Ruđer Bošković Institute, Croatia
2. Department of Functional and Evolutionary Ecology, University of Vienna, Austria
3. Department of Marine Microbiology and Biogeochemistry, Royal Netherlands Institute for Sea Research (NIOZ), Utrecht University, The Netherlands

*To whom correspondence should be addressed:

Marino Korlević

G. Paliaga 5, 52210 Rovinj, Croatia

Tel.: +385 52 804 768

e-mail: marino.korlevic@irb.hr

1 Abstract

2 Background Seagrass meadows are highly productive ecosystems that are considered hotspots for
3 carbon sequestration. The decline of seagrass meadows of various species has been documented
4 worldwide, including that of *Cymodocea nodosa*, a widespread seagrass in the Mediterranean
5 Sea. To assess the influence of seagrass decline on the metabolic profile of sediment microbial
6 communities, metaproteomes from two sites, one without vegetation and one with a declining
7 *Cymodocea nodosa* meadow, were characterised at monthly intervals from July 2017 to October
8 2018.

9 Results The differences in the metabolic profile observed between the vegetated and nonvegetated
10 sediment before the decline were more pronounced in the deeper parts of the sediment and
11 disappeared with the decay of the roots and rhizomes. During the decline, the protein richness
12 and diversity of the metabolic profile of the microbial communities inhabiting the nonvegetated
13 sediment became similar to those observed for the vegetated communities. Temporal shifts in the
14 structure of the metabolic profile were only observed in the nonvegetated sediment and were also
15 more pronounced in the deeper parts of the sediment. The assessment of the dynamics of proteins
16 involved in the degradation of organic matter, such as ABC transporters, fermentation-mediating
17 enzymes, and proteins involved in dissimilatory sulphate reduction, reflected the general dynamics
18 of the metabolic profile.

19 Conclusions Overall, the metabolic profile of the microbial communities inhabiting the nonvegetated
20 sediment was influenced by the decline of seagrass, with stronger shifts observed in the deeper parts
21 of the sediment.

22 Keywords sediment microbial communities, *Cymodocea nodosa*, seagrass meadow decline,
23 northern Adriatic Sea, metaproteomics, microbial metabolic profile

24 **Background**

25 Marine sediments cover around 70 % of the Earth's surface [1]. The biomass in these habitats
26 consists mainly of prokaryotes, whose richness and abundance are comparable to that in the water
27 column [1–3]. The main factor determining the abundance and activity of these microorganisms is
28 the availability of organic matter [3–5]. Coastal waters supply large amounts of organic matter to
29 the underlying sediments, which leads to the consumption of oxygen in the upper centimetres of the
30 sediment and causes anoxic conditions in the deeper sediment [6]. The complete mineralisation of
31 organic compounds in these anoxic environments requires complex microbial interactions [7–9].
32 The stepwise degradation of organic matter begins with the breakdown of complex organic polymers
33 such as carbohydrates or proteins by extracellular enzymes that can be released into solution or
34 remain associated with the cell. These enzymes convert high-molecular-weight organic matter to
35 substrates that are small enough to be transported into the cell [10]. Part of these hydrolytic products
36 are fermented to short-chain fatty acids (SCFAs) and alcohols that facilitate anaerobic microbial
37 respiration, e.g. by sulphate-reducing bacteria or methanogens [8, 9].

38 Shallow coastal sediments colonised by seagrasses are considered a special type of habitat
39 for marine prokaryotes [11]. Such areas are hotspots for microbial activity, as seagrasses enrich
40 the sediment with organic matter by excreting organic carbon, trapping organic particles from the
41 water column, and stabilising the sediment. In addition, the decomposition of seagrass leaves, roots,
42 and rhizomes, which is particularly evident during the decline of the meadows, contributes to the
43 enrichment of the sediment with organic matter [11–14]. Consequently, microbial communities in
44 seagrass sediments are metabolically more diverse and active than those inhabiting bare sediments
45 [15]. Furthermore, taxonomic analyses showed differences between communities at vegetated and
46 nonvegetated sites [16–21] and indicated that microbial communities even differ with respect to
47 the meadow edge [22]. The few available studies on microbial community succession in seagrass
48 sediments suggest changes in sulphate-reducing bacteria over time [23], as well as community
49 changes in response to nutrient availability [24] and seagrass restoration [25]. However, there is not

50 much information on the response of sediment microbial communities to seagrass decline. About
51 19 % of seagrass meadows worldwide have been lost since 1880 [26]. A decline of *Cymodocea*
52 *nodosa*, a widespread and common seagrass species throughout the Mediterranean Sea [27], has
53 been observed [28–31], including in the northern Adriatic Sea [32–34]. In a previous study, we
54 investigated the diversity and dynamics of sediment microbial communities during the decline of
55 the seagrass species *C. nodosa* and found a notable compositional stability in response to such a
56 major disturbance [21].

57 In order to obtain a comprehensive overview of the microbial communities living in sediments
58 colonised by seagrasses, methods that allow functional characterisation, such as metaproteomics,
59 must be applied. This high-throughput “meta-omics” approach is emerging as an important tool
60 for deciphering the key components that determine the function of microbial ecosystems [35]. In
61 addition, this approach has the potential to provide insights into the biogeochemical cycling in marine
62 sediments and to assess the response of microbes to environmental change [36]. Metaproteomics
63 is closely linked to metagenomics, as genome information in combination with data on expressed
64 proteins not only provides information on the functional potential of microbial populations, but
65 also on which metabolism is active in an ecosystem [37]. Metaproteomics has already been used to
66 analyse microbial metabolic processes in cold seeps [38, 39], diffuse hydrothermal venting [40],
67 mudflat aquaculture [41], and chronically petroleum-polluted [42] sediments. To our knowledge
68 there are no metaproteomic studies on microbial communities in seagrass meadow sediments. The
69 aim of the present study was to use a metaproteomic approach to characterise the metabolic profile
70 of prokaryotic communities in *C. nodosa* meadow sediments and to determine the shifts in their
71 metabolic profile when seagrass meadows decline.

72 **Methods**

73 **Sampling**

74 Sediment sampling for DNA and protein isolation was performed as described in Markovski
75 et al. (2022) [21]. For a detailed description of the sampling site, environmental conditions, and
76 the decline of the *C. nodosa* meadow, see Najdek et al. (2020) [34]. In brief, sediment cores were
77 collected from a declining *C. nodosa* meadow (vegetated site) in the Bay of Saline ($45^{\circ}7'5''$ N,
78 $13^{\circ}37'20''$ E) in the northern Adriatic Sea. An adjacent area without seagrass (nonvegetated site)
79 was also sampled. Samples were taken monthly from July 2017 to October 2018. The meadow
80 began to decline in November 2017, and by the end of the study, only small patches of seagrass
81 along the shoreline indicated its former existence. Prior to DNA and protein isolation, the sediment
82 cores were cut into four sections, each 1 cm long: the top (0 – 1 cm), the bottom (7 – 8 cm), and two
83 middle sections: upper middle (2 – 3 cm) and lower middle (3 – 6 cm; Supplementary Table S1).

84 **DNA isolation**

85 Total DNA from each sediment section was isolated using a modified isolation protocol [43]
86 based on Zhou et al. (1996) [44] as described in Markovski et al. (2022) [21]. In brief, 2 g of
87 sediment were weighed, avoiding roots and rhizomes in vegetated cores, mixed with the extraction
88 buffer and proteinase K, and incubated by horizontal shaking at 37°C for 30 min. After the addition
89 of SDS, the mixture was incubated again by horizontal shaking at 65°C for 60 min. The sediment
90 particles were removed by centrifugation and the supernatant was extracted three times with an
91 equal volume of chloroform:isoamyl alcohol (1:1). DNA precipitation was performed by adding
92 isopropanol and incubating the mixture at 22°C for 60 min. The DNA pellet obtained after the
93 centrifugation step was washed twice with cold (-20°C) 70 % ethanol, air-dried, and resuspended
94 in 100 μl of deionised water.

95 **Metagenomics**

96 Due to the limited number of sediment metagenomes that could have been sequenced, we
97 selected four DNA samples from Markovski et al. (2022) [21] collected in August 2018 from
98 the top (0 – 1 cm) and lower middle (4 – 5 cm) layers of both the vegetated and nonvegetated
99 sites (Supplementary Table S2). These selected DNA samples were sent on dry ice to IMGM
100 Laboratories (Martinsried, Germany) for metagenomic sequencing. The genomic DNA was purified
101 using AMPure XP Beads (Beckman Coulter, USA) at a bead:DNA ratio of 1:1 (v/v) and quantified
102 using the Qubit dsDNA HS Assay Kit (Thermo Fisher Scientific, USA). The integrity of the DNA
103 was checked on a 1 % agarose gel. Metagenomic sequencing libraries were prepared from 100 or
104 300 ng of genomic DNA using the NEBNext Ultra II FS DNA Library Prep Kit for Illumina (New
105 England Biolabs, USA) according to the manufacturer's protocol. Fragments of 500 – 700 bp were
106 selected using the AMPure XP Beads, enriched by PCR for 5 or 6 cycles, and quality controlled.
107 The individual libraries generated from different DNA input samples were pooled and sequenced on
108 an Illumina NovaSeq 6000 sequencing system (2 × 250 bp).

109 The sequences obtained were analysed on the Life Science Compute Cluster (LiSC; CUBE
110 – Computational Systems Biology, University of Vienna). MEGAHIT (version 1.2.9) [45], with
111 default settings, was used to assemble individual metagenomic libraries and putative genes were
112 predicted from contigs longer than 200 bp using Prodigal (version 2.6.3) [46] in metagenome mode
113 (-p meta). Predicted genes were functionally annotated using the eggNOG mapper (version 2.1.9)
114 [47] with the eggNOG database (version 5.0.2) [48]. Taxonomic classification was performed
115 using the lowest common ancestor algorithm from DIAMOND (version 2.0.15) [49] against the
116 non-redundant NCBI database (NR). Phylogeny was determined using the top 10 % of hits with
117 an e-value < 1 × 10⁻⁵ (--top 10). Sequence renaming and the calculation of metagenomic statistics
118 were performed using the tools from BBTools (<https://jgi.doe.gov/data-and-tools/bbtools>). In
119 total, metagenomic sequencing generated between 205,085,833 and 216,556,629 sequence pairs
120 (Supplementary Table S2). After the removal of low-quality reads, sequences were assembled

₁₂₁ into 21,634,340 to 33,248,196 contigs, with L50 ranging from 590 to 601 bp. Coding sequence
₁₂₂ (CDS) prediction generated between 27,526,969 and 42,249,295 CDSs, while functional annotation
₁₂₃ resulted in 19,599,377 to 29,892,039 annotated CDSs.

₁₂₄ **Protein isolation**

₁₂₅ The proteins were isolated from the same sediment sections that were used for DNA isolation
₁₂₆ [21]. The SDS-based lysis method with trichloroacetic acid (TCA) precipitation described in
₁₂₇ Chourey et al. (2010) [50] and modified by Hultman et al. (2015) [51] was used. To 5 g of sediment,
₁₂₈ 10 % (w/w) polyvinylpolypyrrolidone (PVPP) was added. The mixture was suspended in 5 ml
₁₂₉ protein extraction buffer (4 % SDS and 100 mM Tris-HCl [pH 8.0]) and vortexed. After incubation
₁₃₀ in boiling water for 5 min, the samples were sonicated and incubated again in boiling water for 5
₁₃₁ min. Sonication was performed using the Sonopuls HD 4100 probe sonicator (Bandelin, Germany)
₁₃₂ equipped with an UW 100 ultrasonic transducer and a TS 103 probe. The solution was sonicated
₁₃₃ at 75 % of the maximum amplitude (245 µm) for 2 min at an interval of 10 s on and 10 s off. The
₁₃₄ sediment particles were removed by centrifugation for 20 min at 4 °C and 4,500 × g. The supernatant
₁₃₅ was transferred to a clean tube and mixed with 1 M dithiothreitol (DTT; final concentration 24 mM).
₁₃₆ The proteins were precipitated with cold (4 °C) 100 % TCA (final concentration 20 %) overnight
₁₃₇ at –20 °C. The protein pellet was obtained by centrifugation for 40 min at 4 °C and 10,000 × g.
₁₃₈ The obtained pellet was washed three times with cold (–20 °C) acetone and centrifuged after each
₁₃₉ washing step for 5 min at 4 °C and 20,000 × g. The pellet was transferred to a clean 1.5 ml tube
₁₄₀ during the first washing step. The dried pellet was stored at –80 °C until further processing. In total,
₁₄₁ 120 protein samples were isolated.

142 Metaproteomics

143 The filter-aided sample preparation (FASP) [52] procedure was used to perform trypsin
144 digestion. Isolated proteins were processed using the FASP Protein Digestion Kit (Expedeon,
145 UK) according to the manufacturer's instructions, with minor modifications [53]. Briefly, the
146 protein pellet was solubilised in the urea sample buffer included in the kit, amended with DTT,
147 and centrifuged to remove larger particles. The trypsin digestion was performed on the column
148 filter overnight at 37 °C for 18 h. The resulting filtrate containing peptides was acidified to a final
149 concentration of 1 % trifluoroacetic acid (TFA). Digested peptides were desalted using the Pierce
150 C18 Tips (Thermo Fisher Scientific, USA) according to the manufacturer's instructions and sent to
151 the Proteomics Facilities of the University of Vienna for mass spectrometry analysis.

152 MS/MS spectra were obtained using a Q Exactive Hybrid Quadrupole-Orbitrap Mass
153 Spectrometer (Thermo Fisher Scientific, USA) and searched against a protein database containing
154 amino acid sequences of predicted CDSs from combined metagenomes that were sequenced
155 and analysed as described above. MS/MS spectra were successfully generated for 118 samples
156 (Supplementary Table S1). Before the protein database search, the predicted CDSs were clustered
157 at 90 % similarity using CD-HIT (version 4.6.8). Peptides were identified using the SEQUEST-HT
158 engine and validated with Percolator, all within Proteome Discoverer (version 2.1; Thermo Fisher
159 Scientific, USA). The probability of false peptide identification was reduced by applying the
160 target-decoy approach. Only peptides with a false discovery rate < 1 % were retained. Protein
161 identification required at least two peptides, including one unique peptide. Quantification of the
162 relative abundance of proteins was conducted using a chromatographic peak area-based label-free
163 quantitative method [54, 55], where the peak areas of unique peptides were summed and normalised
164 to the normalised area abundance factor (NAAF). In total, 67,947 different proteins were identified
165 from the obtained MS/MS spectra. Of all identified proteins, 94.6 % were annotated by the
166 eggNOG database. To focus exclusively on microbial communities, only proteins classified as
167 *Archaea* and *Bacteria* using the NCBI database were retained. As a precautionary measure, proteins

¹⁶⁸ that were not taxonomically classified as *Archaea* or *Bacteria* by the eggNOG database were also
¹⁶⁹ removed, leaving a total of 57,305 proteins in the dataset.

¹⁷⁰ **Data analysis**

¹⁷¹ Data processing and visualisation were performed using R (version 4.4.2) [56] combined with
¹⁷² the tidyverse package (version 2.0.0) [57, 58] and several other packages [59–78]. The Shannon
¹⁷³ diversity index was calculated using the function `diversity` from the vegan package (version 2.6.4)
¹⁷⁴ [71]. To express the diversity index in terms of the effective number of proteins, the exponential
¹⁷⁵ of the Shannon diversity index was calculated [79]. Differences between the number of observed
¹⁷⁶ proteins, the exponential of the Shannon diversity index, and the NAAFs between sites, sediment
¹⁷⁷ layers, i.e., sections of sediment cores, and the period before and during the decay of *C. nodosa* roots
¹⁷⁸ and rhizomes were tested by applying the Mann-Whitney *U* test using the function `wilcox.test`
¹⁷⁹ [56]. The Bonferroni correction was applied to solve the problem of multiple comparisons using the
¹⁸⁰ function `p.adjust` [56]. Differences in the structure of the microbial metabolic profiles between
¹⁸¹ sites, sediment layers, and the period before and during the decay of *C. nodosa* roots and rhizomes
¹⁸² were tested on Bray-Curtis dissimilarities based on protein NAAFs by performing the Analysis of
¹⁸³ Similarities (ANOSIM) using the function `anosim` from the vegan package and 999 permutations
¹⁸⁴ [71]. The grouping of samples into the period before and during the decay of roots and rhizomes
¹⁸⁵ was based on the decline of *C. nodosa* reported by Najdek et al. (2020) [34]. The sampling period
¹⁸⁶ from the beginning of the study until February 2018 was labelled the period before the decay of
¹⁸⁷ roots and rhizomes, while the period after this month was referred to as the period of decay of roots
¹⁸⁸ and rhizomes. Principal Coordinate Analysis (PCoA) was performed on Bray-Curtis dissimilarities
¹⁸⁹ based on protein NAAFs using the function `wcmdscale` from the vegan package. If necessary, the
¹⁹⁰ Lingoes correction method was applied to account for negative eigenvalues [71, 80, 81].

191 **Results**

192 To assess the richness and diversity of isolated proteins from the sediment microbial
193 communities in the Bay of Saline, the number of observed proteins and the exponential of the
194 Shannon diversity index were calculated. Samples from each layer were grouped based on
195 the sampling site and the period before and during the decay of *C. nodosa* roots and rhizomes.
196 Comparisons between sampling sites in each period and between different periods at each site were
197 performed (Fig. 1). In all layers, significantly ($p < 0.05$) higher numbers of observed proteins were
198 found during the period before the decay of roots and rhizomes at the vegetated (top, 35,626 –
199 37,937 proteins; upper middle, 32,494 – 39,996 proteins; lower middle, 35,220 – 39,713 proteins;
200 and bottom, 32,183 – 37,440 proteins) compared to the nonvegetated (top, 29,217 – 36,284 proteins;
201 upper middle, 29,312 – 36,755 proteins; lower middle, 25,752 – 33,630 proteins; and bottom,
202 27,672 – 33,922 proteins) site. In contrast, no significant changes between sites were observed
203 in all layers during the period of roots and rhizomes decay. In addition, no significant changes
204 were found at each site between the two periods. When analysing the exponential of the Shannon
205 diversity index, significant changes were observed only in the lower middle and bottom layer (Fig.
206 1). Here, in agreement with the number of observed proteins, higher values were found during the
207 period before the decay of roots and rhizomes at the vegetated (lower middle 7,594.2 – 11,300.0
208 proteins and bottom, 3,927.3 – 10,300.9 proteins) compared to the nonvegetated site (lower middle
209 1,497.2 – 3,070.7 proteins and bottom, 586.6 – 2,696.5 proteins). Also, in agreement with the
210 number of observed proteins, no significant changes were observed between the sites during the
211 period of roots and rhizomes decay. Additionally, the Shannon diversity index showed significant
212 changes in these layers between the two periods. In the lower middle layer of the vegetated site,
213 significantly higher values were observed before (7,594.2 – 11,300.0 proteins) than during (4,254.3
214 – 9,227.5 proteins) roots and rhizomes decay. However, in the bottom layer of the nonvegetated site
215 significantly higher values were found during the period of roots and rhizomes decay (1,815.8 –
216 6,775.9 proteins) than before the decay (586.6 – 2,696.5 proteins).

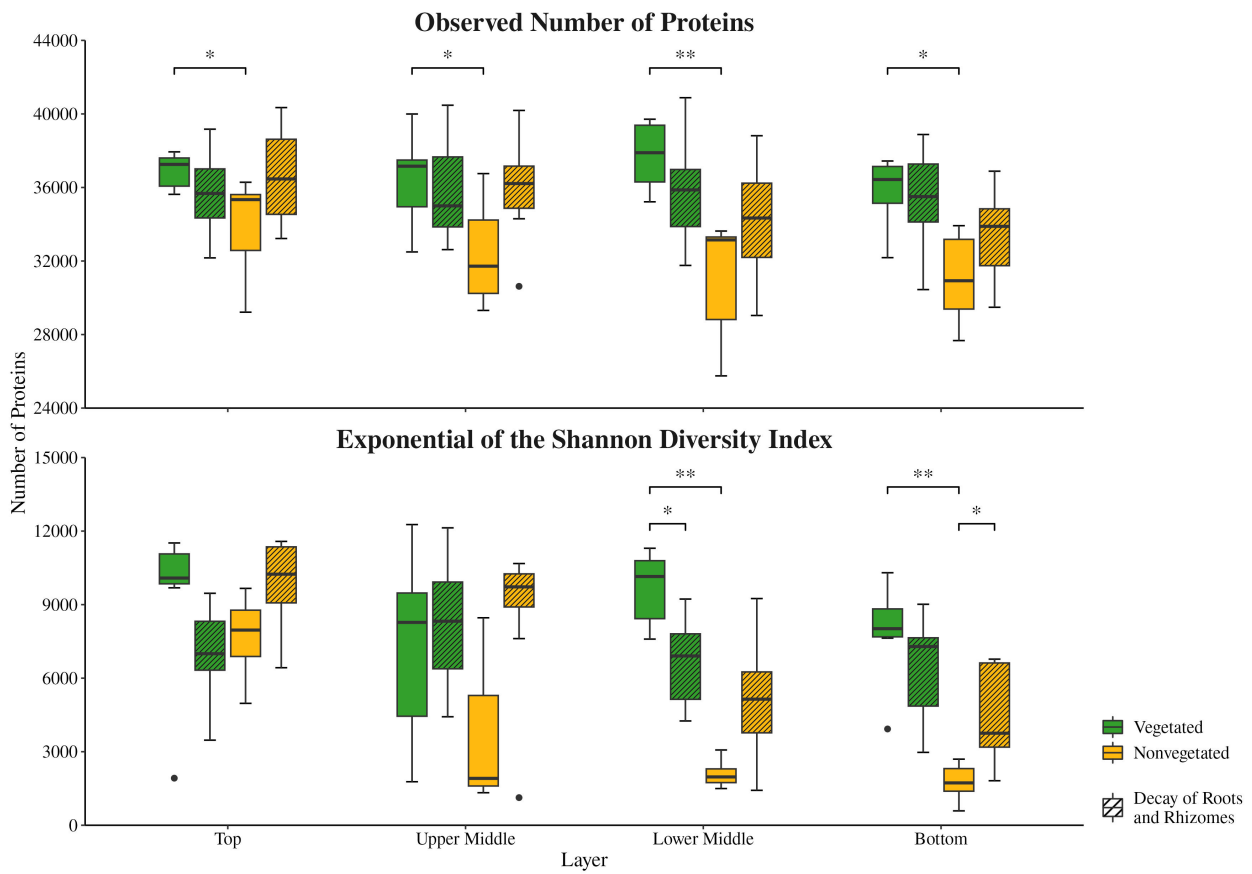


Fig. 1 The observed number of proteins and the exponential of the Shannon diversity index of sediment microbial communities in the Bay of Saline. Samples were collected in different sediment layers at the vegetated and nonvegetated site before and during the decay of roots and rhizomes of *C. nodosa*. Asterisks indicate the level of statistical significance: * $p < 0.05$ and ** $p < 0.01$.

217 ANOSIM testing of Bray-Curtis dissimilarities was applied to determine the changes in the
 218 structure of the metabolic profile of the sediment microbial communities. When all proteins from
 219 all samples were analysed together, no strong differentiation was observed between sites, layers,
 220 or the period before and during the decay of roots and rhizomes (ANOSIM, $R = 0.14 - 0.24$, all
 221 $p < 0.01$). To determine whether only a part of the metabolic network showed any differentiation,
 222 proteins classified in the Cluster of Orthologous Genes (COG) category C (energy production and
 223 conversion), the most abundant category in our samples (see below, Supplementary Table S3), were
 224 analysed separately. However, no strong differentiation was observed between sites, layers, or decay
 225 periods when only these proteins were considered (ANOSIM, $R = 0.15 - 0.21$, all $p < 0.01$). In

addition, the separate analysis of samples from the vegetated and nonvegetated site of all and COG C categorised proteins did also not reveal a strong differentiation between layers or decay periods (ANOSIM, $R = 0.09 - 0.26$, all $p < 0.01$), with the exception of a more pronounced separation observed at the nonvegetated site between the periods before and during the decay of roots and rhizomes. This separation could be observed when all proteins (ANOSIM, $R = 0.33$, $p < 0.01$) and, especially, when proteins from the functional COG category C (ANOSIM, $R = 0.51$, $p < 0.01$) were considered. To gain a clearer overview of this separation, samples from the nonvegetated site were analysed using PCoA (Fig. 2). A distinction of samples from the lower middle and bottom layer retrieved during the period before the decay of roots and rhizomes from all other samples was noticed. This distinction could be observed when all proteins were analysed together, but especially when proteins from the functional COG category C were considered (Fig. 2). Furthermore, to gain a better insight in the change of the structure of the metabolic profile between the period before and during the decay of roots and rhizomes, samples from each site and layer were analysed separately. Sediment layers of the vegetated site did not show any strong differentiation between these two periods when either all (ANOSIM, $R = 0.05 - 0.31$, $p = 0.01 - 0.23$) or only COG C categorised proteins (ANOSIM, $R = 0.12 - 0.30$, $p = 0.01 - 0.05$) were considered. In contrast, a pronounced separation between the two periods was observed in different layers of the nonvegetated site (Fig. 3). When comparing the layers of this site, the lowest distinction between the two periods was observed in the top layer (ANOSIM; all proteins, $R = 0.35$, $p < 0.01$; COG C proteins, $R = 0.38$, $p < 0.01$), middle in the upper and lower middle layer (ANOSIM; all proteins, $R = 0.29 - 0.45$, all $p < 0.01$; COG C proteins, $R = 0.53 - 0.62$, all $p < 0.01$), and the highest in the bottom layer (ANOSIM; all proteins, $R = 0.53$, $p < 0.01$; COG C proteins, $R = 0.95$, $p < 0.01$).

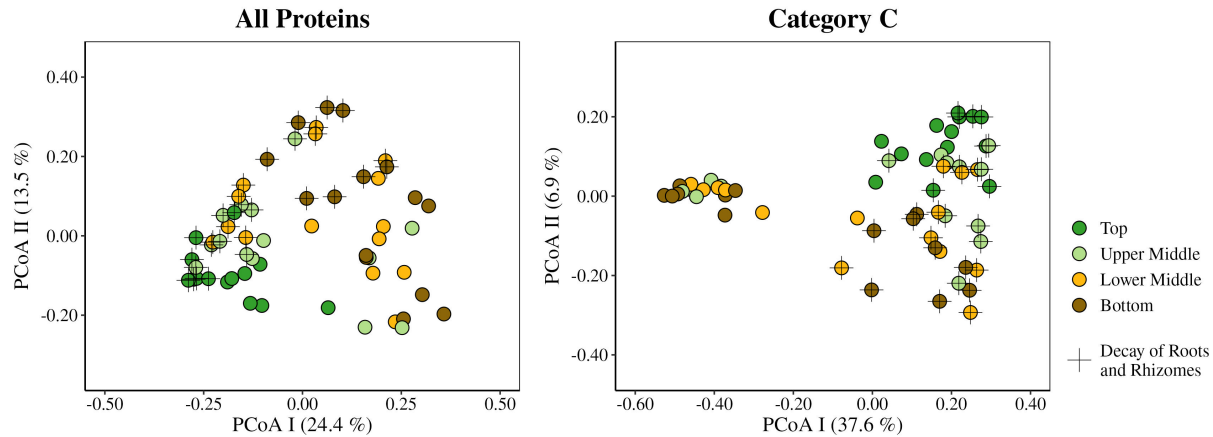


Fig. 2 PCoA of Bray-Curtis dissimilarities of microbial proteins sampled in the sediment of the Bay of Saline. All proteins and proteins classified only into COG category C (energy production and conversion) were analysed. Only samples collected in sediment layers at the nonvegetated site before and during decay of roots and rhizomes of *C. nodosa* are shown. The proportion of variation explained by each axis is indicated in parentheses on the corresponding axis.

248 A total of 52,270 different proteins were assigned to a COG functional category. The most
 249 abundant COG category in terms of the number of proteins it contained (8,224 proteins) and
 250 their NAAFs (15.2 %) was the functional COG category C, which comprises proteins for energy
 251 production and conversion (Supplementary Table S3). To detect how the decay of the meadow
 252 affected the energy production and conversion of sediment microbial communities in the Bay of
 253 Saline, we assessed the NAAF dynamics of the functional COG category C in each sediment layer.
 254 When comparing the sites before the decay of roots and rhizomes, significant ($p < 0.05$) differences
 255 were only observed in the bottom layer where the proteins of this functional category comprised
 256 a larger proportion at the nonvegetated (19.5 – 31.7 %) than at the vegetated (13.8 – 26.2 %) site.
 257 No significant difference was found between the sites during the decay period. When comparing
 258 the layers of the individual sites before and during the decay of roots and rhizomes, we detected a
 259 significant change in the proportion of the functional COG category C only in the bottom layer of
 260 the nonvegetated site. Here, a significant decrease in the proportion of this functional category was
 261 observed between the period before (19.5 – 31.7 %) and during (8.2 – 13.9 %) the decay of roots
 262 and rhizomes.

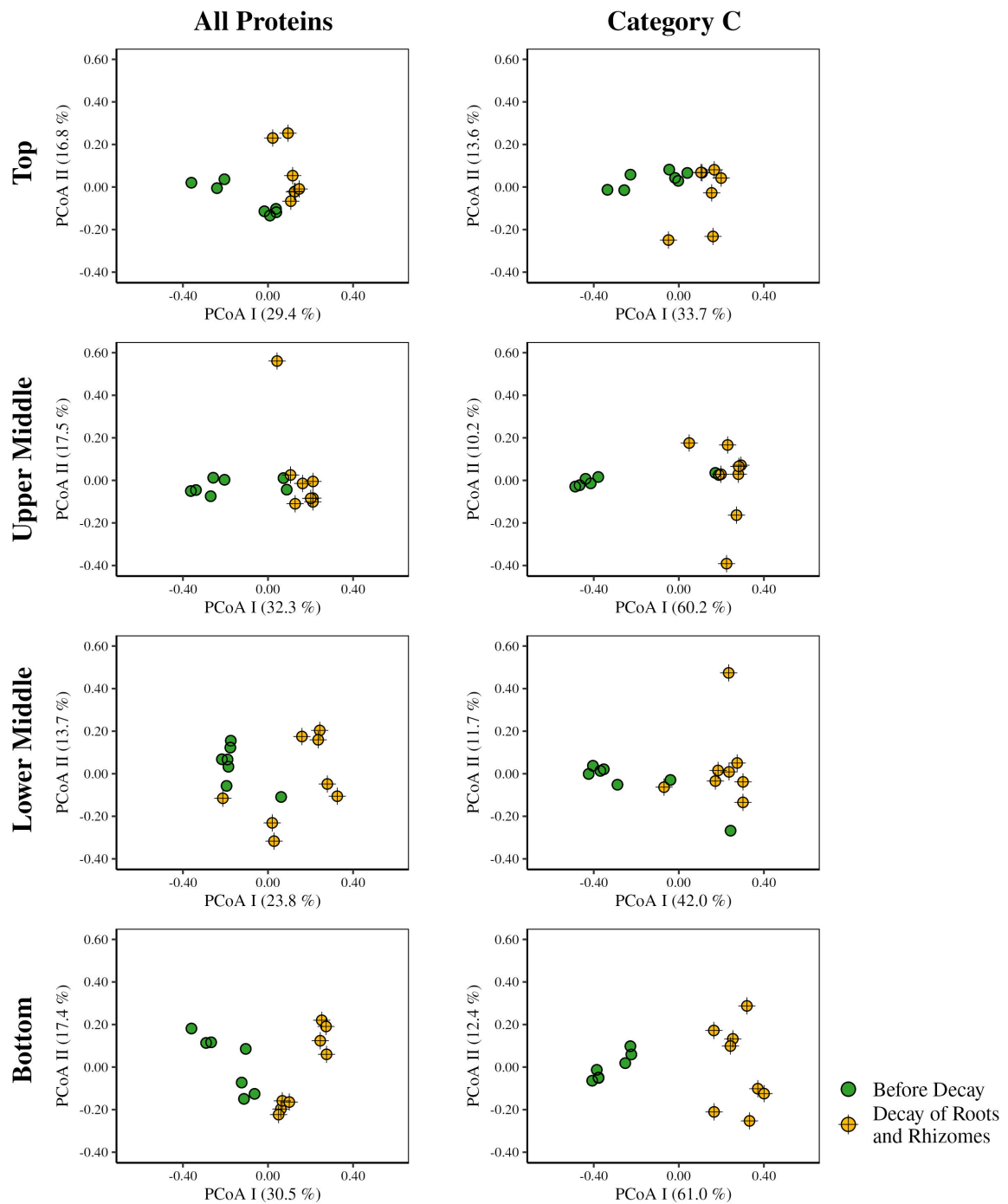


Fig. 3 PCoA of Bray-Curtis dissimilarities of microbial proteins sampled in each layer in the sediment of the Bay of Saline. All proteins and proteins classified only into COG category C (energy production and conversion) were analysed. Only samples collected at the nonvegetated site before and during decay of roots and rhizomes of *C. nodosa* are shown. The proportion of variation explained by each axis is indicated in parentheses on the corresponding axis.

As the COG categories provide only a broad overview, the predicted CDSs were also classified using the Kyoto Encyclopaedia of Genes and Genomes (KEGG) Orthology (KO) database to gain better insight into the metabolic profile. A total of 1,408 different KO entries were present in the dataset, while 37,243 proteins were assigned to one or more of these KO entries. As the functional COG category C was the most abundant in our dataset (Supplementary Table S3), we aimed to further explore the dynamics of the most pronounced KO entries within this category. The F-type H⁺-transporting ATPase subunit c (ATPF0C, atpE; 20.0 %), the K⁺-stimulated pyrophosphate-energized sodium pump (hppA; 7.9 %), and the adenylylsulphate reductase subunits A (aprA; 6.2 %) and B (aprB; 6.1 %) represented the highest proportion (NAAF) within the functional COG category C (Fig. 4). As the samples from the nonvegetated site showed a clear separation based on the period of roots and rhizomes decay, especially when the COG category C dataset was considered (Fig. 2), we compared the proportion of these three proteins at the nonvegetated site before and during the decay of roots and rhizomes (Fig. 4). We observed a significant ($p < 0.05$) decrease in the proportion of the F-type H⁺-transporting ATPase subunit c during the decay of roots and rhizomes in all layers. This decrease was particularly pronounced in the bottom layer, where this protein constituted between 52.7 and 76.0 % of all COG C categorised proteins before the decay. During the decay of roots and rhizomes, its proportion dropped to between 3.2 and 19.3 %. Although not as pronounced as the change in the F-type H⁺-transporting ATPase subunit c, the K⁺-stimulated pyrophosphate-energized sodium pump also showed a significant shift between the two periods in all layers, except the top layer. The most significant shift was observed in the bottom layer, where this protein increased from between 0.8 and 4.9 % of all COG categorised proteins before the decay to between 4.9 and 11.6 % during the decay ($p < 0.001$). The proportion of the adenylylsulphate reductase subunits A and B also increased during the decay in all layers, with the exception of the top layer. However, this shift was only significant in the bottom layer, where this protein increased from 3.5 to 7.4 % of all COG categorised proteins before the decay to 12.1 to 15.7 % during the decay.

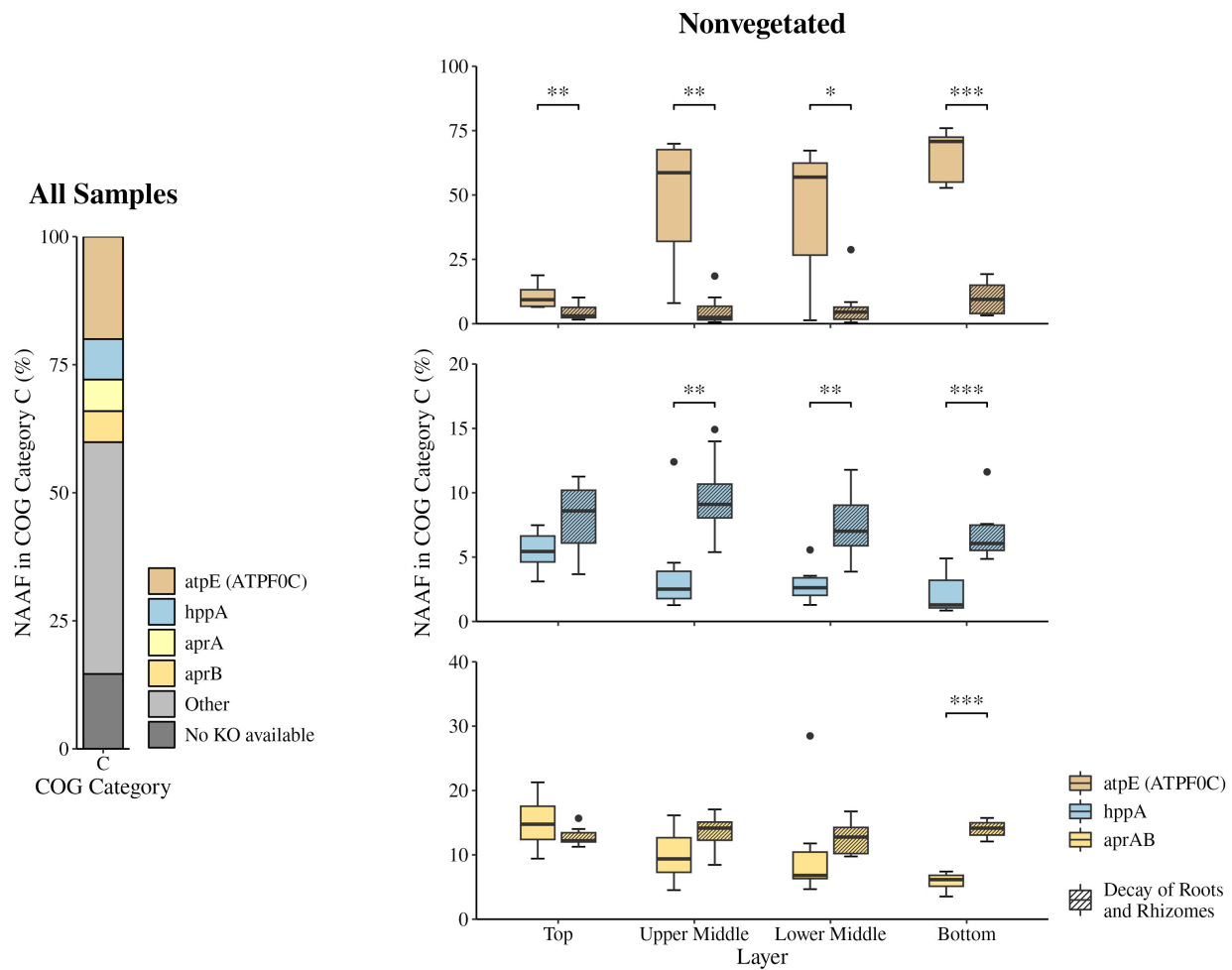


Fig. 4 Proportion of the most abundant (> 3 %) KEGG KO entries within the functional COG category C (energy production and conversion) in all samples and changes in the proportion of the same entries in each layer at the nonvegetated site before and during the decay of roots and rhizomes of *C. nodosa* in the Bay of Saline. The proportion was calculated using the NAAF. Asterisks indicate the level of statistical significance: * $p < 0.05$, ** $p < 0.01$, and *** $p < 0.001$.

289 The degradation of complex organic matter by the sediment microbial community in the
 290 Bay of Saline was evaluated by assessing the dynamics of the carbohydrate, protein, and lipid
 291 hydrolytic enzymes (Fig. 5). The dynamics of carbohydrate hydrolytic enzymes was determined
 292 using Carbohydrate-Active enZymes (CAZymes), whose proportion did not significantly ($p < 0.05$)
 293 change between stations or decay periods, with the exception of the top sediment layer at the
 294 nonvegetated site. Here, a significant decrease in the proportion of CAZymes was observed from
 295 the period before decay (0.28 – 0.43 %) to the period of roots and rhizomes decay (0.22 – 0.28

296 %; Fig. 5). Proteins assigned to the glycoside hydrolase families GH5 and GH9 were the most
297 abundant of all CAZymes (47.2 %). To assess protein degradation, we focused on proteins assigned
298 as peptidases in KEGG. The proportion of these enzymes significantly increased in the upper middle
299 layer of the vegetated site from the period before decay (0.15 – 0.45 %) to the period of roots
300 and rhizomes decay (0.34 – 0.61 %; Fig. 5). Peptidases were almost exclusively comprised of
301 metalloendopeptidases and serine endopeptidases (93.3 %). Compared to CAZymes and peptidases,
302 lipases were the least represented in our data (Fig. 5).

303 We assessed the dynamics of ATP-binding cassette (ABC) transporters to evaluate the uptake of
304 hydrolytic products by prokaryotic cells. Substrate-binding proteins classified as ABC transporters
305 in the KEGG Pathway (map02010) were selected and further manually classified into the following
306 categories based on the molecules they transport: sugar, peptide, amino acid, urea, lipid, polyol,
307 phosphate, and mineral and organic ion (Fig. 5). Sugar (38.0 %) and amino acid (31.5 %)
308 transporters were the most abundant among all selected ABC transporters. In the lower middle and
309 bottom layer, a significantly ($p < 0.05$) higher proportion of sugar ABC transporters was observed at
310 the vegetated (lower middle, 2.90 – 4.57 %; bottom, 3.90 – 5.52 %) than at the nonvegetated (lower
311 middle, 2.25 – 3.20 %; bottom, 1.75 – 2.81 %) site during the period before roots and rhizomes decay
312 (Fig. 5). In contrast, no significant differences in the proportion of ABC transporters targeting sugars
313 between sites were observed during the period of roots and rhizomes decay. These transporters also
314 showed a significant increase in the bottom layer of the nonvegetated site from the period before
315 decay (1.75 – 2.81 %) to the period of roots and rhizomes decay (2.16 – 6.79 %). The proportion
316 of ABC transporters targeting amino acids only showed a significant increase in the bottom layer
317 of the nonvegetated site from the period before decay (2.05 – 3.02 %) to the period of roots and
318 rhizomes decay (2.76 – 4.62 %).

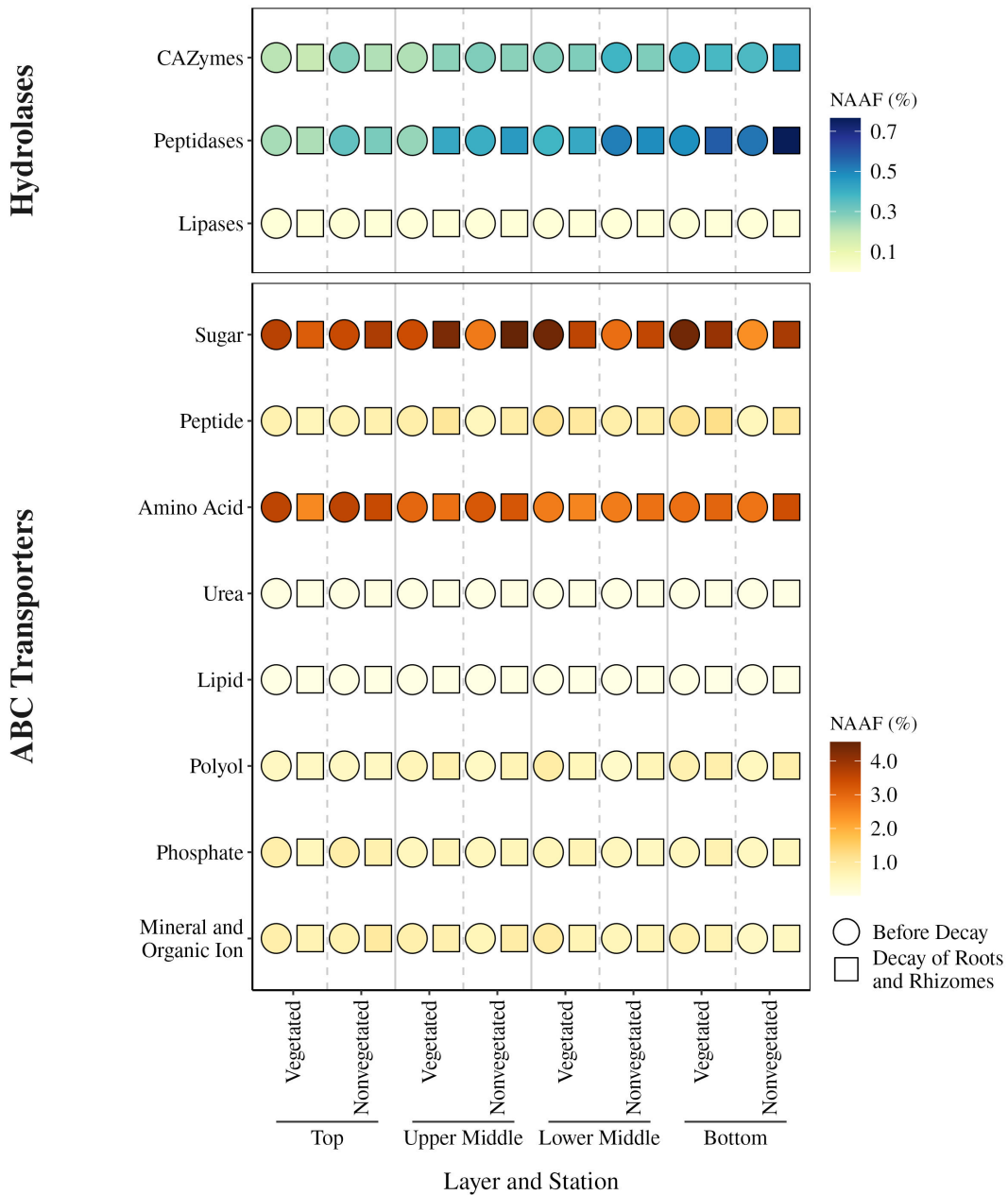


Fig. 5 Median proportion of groups of hydrolases and ABC transporters in sediment layers at the vegetated and nonvegetated site before and during the decay of roots and rhizomes of *C. nodosa* in the Bay of Saline. The proportion was calculated using the NAAF.

319 To evaluate the role of fermentation processes at these two sites, we selected enzymes from
 320 the KEGG database that are thought to be involved in mediating various fermentation products
 321 such as carbon dioxide, formate, acetate, acetone, ethanol, lactate, acetooin, propionate, and butyrate

322 (Supplementary Table S4). Of these selected enzymes, our dataset contained pyruvate:ferredoxin
323 oxidoreductase, pyruvate formate-lyase, acetyl-CoA hydrolase, acetate kinase, and alcohol, formate,
324 and lactate dehydrogenase (Fig. 6). Formate dehydrogenase (45.2 %), pyruvate:ferredoxin
325 oxidoreductase (31.4 %), and alcohol dehydrogenase (17.0 %) were the most prominent of all
326 fermentation-mediating enzymes detected. Significantly ($p < 0.05$) higher proportions of formate
327 dehydrogenase were detected before the decay of roots and rhizomes in the lower middle layer
328 of the vegetated (0.28 – 0.45 %) compared to the nonvegetated (0.20 – 0.30 %) site. In contrast,
329 no significant differences were observed during the decay of roots and rhizomes. A similar trend
330 was observed for pyruvate:ferredoxin oxidoreductase in the bottom layer, which had a higher
331 proportion of this enzyme before the decay of roots and rhizomes at the vegetated (0.14 – 0.30 %)
332 compared to the nonvegetated (0.09 – 0.22 %) site. However, no significant differences between
333 sites were observed during the decay of roots and rhizomes (Fig. 6). Alcohol dehydrogenase showed
334 significant differences between sites in both the lower middle and bottom layer. In the lower middle
335 layer, a higher proportion of this enzyme was observed at the vegetated than at the nonvegetated
336 site before (vegetated, 0.08 – 0.16 %; nonvegetated; 0.04 – 0.07 %) and during the decay of roots
337 and rhizomes (vegetated, 0.07 – 0.43 %; nonvegetated; 0.04 – 0.11 %). The same pattern of higher
338 proportions of this enzyme at the vegetated site before (vegetated, 0.08 – 0.26 %; nonvegetated;
339 0.05 – 0.07 %) and during roots and rhizomes decay (vegetated, 0.13 – 0.88 %; nonvegetated; 0.06 –
340 0.14 %) was also detected in the bottom layer.

341 To obtain an overview of the different microbial metabolic processes occurring in the sediment
342 of the Bay of Saline, we selected KEGG modules describing methane-, nitrogen-, and sulphur-related
343 processes (Supplementary Table S5). Among all tested modules we found proteins involved
344 in the following processes: methanogenesis, nitrogen fixation, dissimilatory nitrate reduction,
345 denitrification, assimilatory and dissimilatory sulphate reduction, and thiosulphate oxidation by
346 the SOX complex. Since one of the most prominent proteins in the functional COG category
347 C (energy production and conversion) was the adenylylsulphate reductase (Fig. 4), which is
348 involved in dissimilatory sulphate reduction, the dynamics of the enzymes involved in this process

were investigated in more detail. Of the enzymes involved in dissimilatory sulphate reduction, our dataset contained sulphate adenylyltransferase, adenylylsulphate reductase, and dissimilatory sulphite reductase (Fig. 6). The proportion of adenylylsulphate reductase was much higher (75.0 %) than that of sulphate adenylyltransferase (11.1 %) and dissimilatory sulphite reductase (13.9 %). Significantly ($p < 0.05$) higher proportions of sulphate adenylyltransferase were observed before roots and rhizomes decay at the vegetated than at the nonvegetated site in the upper middle (vegetated, 0.18 – 0.55 %; nonvegetated, 0.10 – 0.28 %), lower middle (vegetated, 0.27 – 0.61 %; nonvegetated, 0.06 – 0.19 %), and bottom (vegetated, 0.17 – 0.32 %; nonvegetated, 0.06 – 0.20 %) layer. In addition, significantly higher proportions were also found in the bottom layer of the nonvegetated site during roots and rhizomes decay (0.14 – 0.35 %) compared to the period before the decay (0.06 – 0.20 %). Proportions of the adenylylsulphate reductase showed significant changes in the lower middle layer, where higher values were observed before roots and rhizomes decay at the vegetated (1.99 – 3.05 %) compared to the nonvegetated (1.22 – 2.53 %) site. Also, in the same layer of the vegetated site significantly higher proportions were detected before roots and rhizomes decay (1.99 – 3.05 %) compared to the period of the decay (1.33 – 2.40 %). In the lower middle and bottom layer, dissimilatory sulphite reductase showed higher proportions before roots and rhizomes decay at the vegetated (lower middle, 0.37 – 0.78 %; bottom, 0.25 – 0.42 %) than at the novegetated (lower middle, 0.16 – 0.40 %; bottom, 0.11 – 0.21 %) site. In addition, significantly higher proportions were detected in the bottom layer of the nonvegetated site during roots and rhizomes decay (0.17 – 0.39 %) compared to the period before the decay (0.11 – 0.21 %). In contrast, no significant differences between stations were observed during the decay of roots and rhizomes for either of these enzymes (Fig. 6).

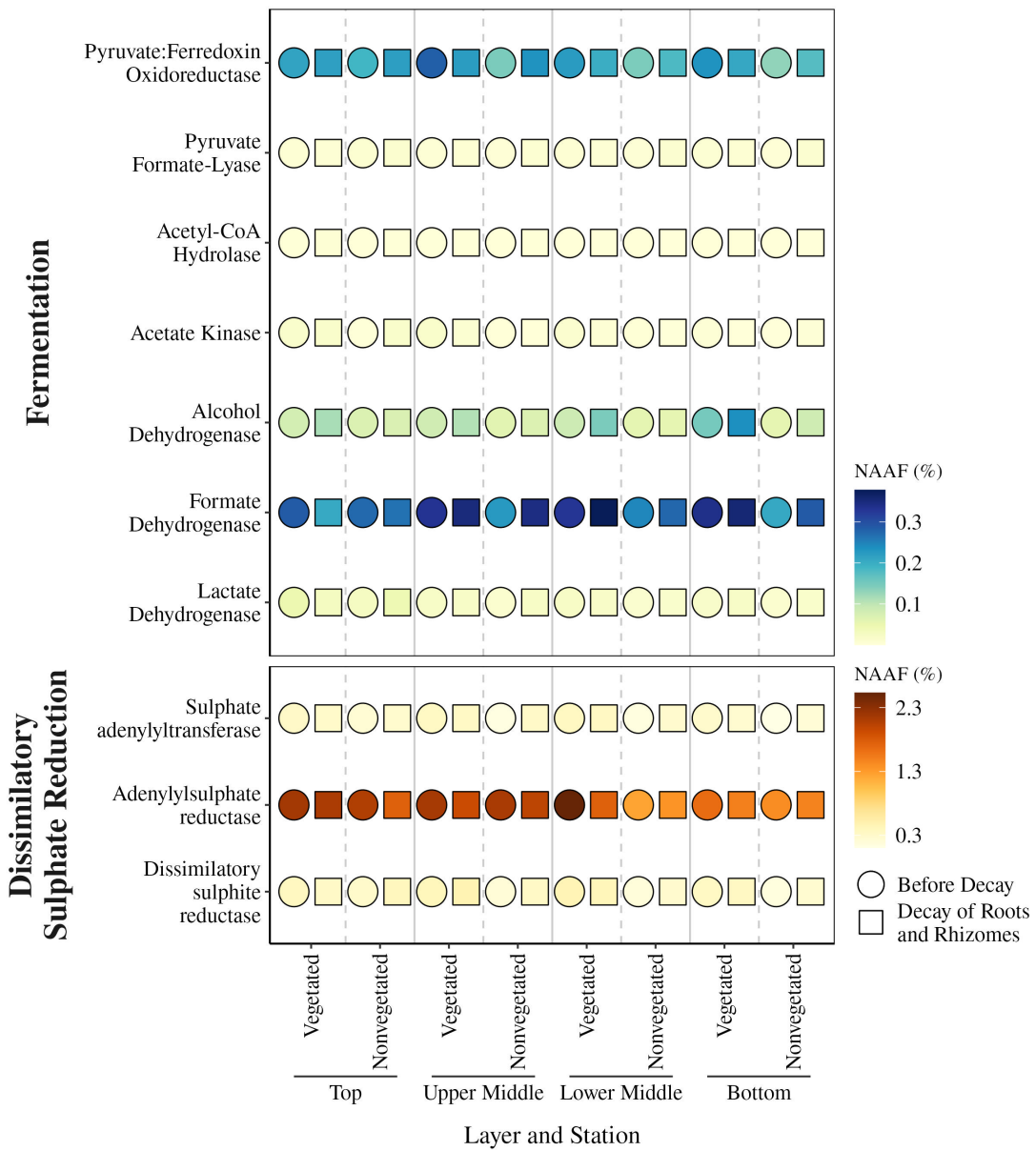


Fig. 6 Median proportion of enzymes involved in mediating various fermentation products and dissimilatory sulphate reduction in sediment layers at the vegetated and nonvegetated site before and during the decay of roots and rhizomes of *C. nodosa* in the Bay of Saline. The proportion was calculated using the NAAF.

371 **Discussion**

372 Seagrass meadow habitats are highly productive ecosystems [82] that support high biodiversity
373 [83]. In the present study, before the decay of the roots and rhizomes of *C. nodosa*, higher values of
374 the number of observed proteins and of the exponential of the Shannon diversity index were found
375 in the vegetated compared to the nonvegetated sediment. These differences were more pronounced
376 in the deeper parts of the sediment (i.e., in the lower middle and bottom layer). After the decay,
377 the differences began to disappear and the values of the number of observed proteins and of the
378 Shannon diversity index were similar to those observed in the sediment previously inhabited by
379 the meadow. In addition, the structure of the metabolic profile of the communities inhabiting the
380 nonvegetated sediment showed a separation between the period before and during the decay of roots
381 and rhizomes, especially in the deeper parts of the sediment and when only proteins for energy
382 production and conversion were considered. This pattern was not observed for the communities at
383 the vegetated site. The difference between the microbial communities inhabiting the vegetated and
384 nonvegetated sediment in the period before roots and rhizomes decay is not surprising, as several
385 studies have found that the presence of seagrass leads to the formation of sediment communities
386 that differ in composition [16–22] and function [15] from communities inhabiting nonvegetated
387 sediments. In addition, the higher values of the number of observed proteins and of the Shannon
388 diversity index at the vegetated site before the decay are consistent with other studies reporting
389 higher metabolic diversity and microbial community activity in seagrass sediments compared to
390 nonvegetated areas and with higher organic matter content in seagrass-inhabited sediments [11, 15].
391 In addition, the greater differentiation observed in the deeper layers in terms of protein richness
392 and diversity is consistent with a previous study on the same sediment communities, which found a
393 greater community separation between sites in the deeper parts of the sediment [21]. In contrast,
394 the less pronounced differentiation observed for the same parameters and for the structure of the
395 metabolic profile in the top and upper middle layer could be explained by the input of organic matter
396 derived from the vegetated site, making the communities in the upper part of the sediment more

³⁹⁷ similar to each other. Indeed, organic matter imported from the seagrass meadow has been shown to
³⁹⁸ be an important source for prokaryotes in nonvegetated sediments [84].

³⁹⁹ The lack of differences between sites during the decay of roots and rhizomes in the number
⁴⁰⁰ of observed proteins and in the exponential of the Shannon diversity index indicates the presence
⁴⁰¹ of a more uniform microbial metabolic profile during this period, similar to the metabolic profile
⁴⁰² observed at the vegetated site prior to decline. This observation is supported by the greater similarity
⁴⁰³ in the structure of the metabolic profile of the communities at the nonvegetated site during decline
⁴⁰⁴ with the metabolic profile of the communities in the upper sediment prior to decline. Because
⁴⁰⁵ seagrass meadows fix the sediment by reducing resuspension rates and sediment mixing [85], we
⁴⁰⁶ hypothesise that resuspension, mixing, and transport between sites are enhanced when the meadow
⁴⁰⁷ is no longer present, allowing greater input of fresh organic matter to the nonvegetated sediment.
⁴⁰⁸ Indeed, Najdek et al. (2020) [34] reported higher levels of total lipids and organic matter at the
⁴⁰⁹ nonvegetated site during the *C. nodosa* decline from May to August 2018. The uniformity of the
⁴¹⁰ microbial profile observed at the vegetated site during the study could be the result of maintaining
⁴¹¹ the source of organic matter during the decline of the seagrass through the decay of leaves, roots,
⁴¹² and rhizomes [11–14].

⁴¹³ The analysis of the functional COG categories showed that category C, which includes
⁴¹⁴ proteins for energy production and conversion, was the most abundant. This is consistent with the
⁴¹⁵ metagenomic study of Habibi et al. (2023) [86], who reported that energy production and conversion
⁴¹⁶ was also one of the most abundant functional COG categories in coastal sediments. Among these
⁴¹⁷ proteins, F-type H⁺-transporting ATPase subunit c, K⁺-stimulated pyrophosphate-energized sodium
⁴¹⁸ pump, and adenylylsulphate reductase subunits A and B exhibited the highest proportion. The
⁴¹⁹ pronounced presence of the F-type H⁺-transporting ATPase subunit c in the deeper parts of the
⁴²⁰ nonvegetated sediment prior to decay could be explained by the involvement of this enzyme in the
⁴²¹ generation of membrane potential. The F-type ATPase can work in both directions, utilising the
⁴²² proton gradient to generate ATP or hydrolysing the ATP to generate the membrane potential [87].

423 The high proportion of the K⁺-stimulated pyrophosphate-energized sodium pump in our dataset
424 indicates the coupling of the energy released by pyrophosphate hydrolysis with the active transport
425 of cations across membranes [88, 89]. The proportion of this protein was increased in the deeper
426 parts of the nonvegetated sediment during decay, reflecting the need of microbial communities
427 for more active cross-membrane transport probably due to the increased input of fresh organic
428 matter from the vegetated site. The high proportion of adenylylsulphate reductase subunits A and B
429 among the proteins for energy production and conversion is not surprising, as this enzyme is part
430 of dissimilatory sulphate reduction to sulphide, a predominant terminal pathway of organic matter
431 mineralisation in anoxic seabeds, where it reduces adenosine-5'-phosphosulphate to sulphite [90].
432 Furthermore, its significantly higher proportion in the nonvegetated sediment during decay could
433 also be explained by the enhancement of this terminal pathway as a result of increased input of
434 fresh organic matter from the vegetated site.

435 High molecular weight organic matter in marine sediments must be converted into low
436 molecular weight molecules by various hydrolytic enzymes so that it can be taken up by cells
437 [10]. Important components of organic matter in coastal marine sediments are carbohydrates,
438 proteins, and lipids [91]. In our dataset, CAZymes and peptidases were more abundant than lipases,
439 which may indicate the importance of carbohydrates and proteins as sources of organic matter for
440 the microbial community. Among the CAZymes, the glycoside hydrolase families GH5 and GH9
441 were the most abundant. These families contain members capable of hydrolysing plant organic
442 matter such as cellulose [92–94]. The presence of enzymes acting on cellulose is not surprising as
443 cellulose is a major component of seagrass cell walls and contributes between 20 and 77 % to the dry
444 plant material [95–97]. Metalloendopeptidases and serine endopeptidases made up the vast majority
445 of peptidases in our dataset. A high proportion of these enzymes among the extracellular proteases
446 has already been reported for coastal sediments [98–100]. CAZymes and peptidases showed no
447 dynamics from pre-decay to decay of roots and rhizomes, except that CAZymes decreased in the
448 top layer of the nonvegetated sediment and peptidases increased in the upper middle layer of the
449 vegetated sediment. Studies have shown that the molar carbon:nitrogen content in seagrass litter

450 decreases during the decomposition process, which could be explained by increased microbial
451 colonisation of detrital matter and microbial utilisation of exogenous nitrogen which could be
452 related to the observed decrease in CAZymes and increase in peptidases [12, 14].

453 Once complex organic compounds have been broken down, the hydrolytic products can be
454 transported into the cells. Prokaryotes utilise various transport proteins, including ABC transporters,
455 to import substrates. Our metaproteomic dataset contained a large amount of ABC transporters for
456 sugars and amino acids. Previous studies of sediment metagenomes also reported a high proportion
457 of ABC transporters [86, 101]. The dynamics of ABC transporters reflected the overall dynamics of
458 the metabolic profile. ABC transporters for sugars showed a higher proportion in the deeper parts
459 of the vegetated compared to the nonvegetated sediment before decay of roots and rhizomes and
460 showed no differences between sites during decay, reflecting the higher organic matter content and
461 corresponding demand for ABC transporters in seagrass-inhabited sediments [11, 15]. In addition,
462 ABC transporters for sugars and amino acids showed an increase in their proportion in the bottom
463 layer of the nonvegetated sediment from the period before decay to the decay of the roots and
464 rhizomes, which could be attributed to changes in organic matter content during the decline of the
465 meadow.

466 The hydrolytic products of the degradation of complex organic matter, such as simple
467 sugars and amino acids, can be imported and consumed by fermenting microbes. We have
468 identified several enzymes involved in mediating various fermentation products, of which formate
469 dehydrogenase, pyruvate:ferredoxin oxidoreductase, and alcohol dehydrogenase are the most
470 abundant. Microcosm studies of the anaerobic degradation of organic matter in marine sediments
471 revealed that acetate, formate, and ethanol are the most common fermentation products [102, 103].
472 In addition, direct measurements of sediment pore water have revealed the presence of methanol and
473 ethanol [104]. It is therefore not surprising that the most common fermentation-mediating enzymes
474 we found are putatively involved in the metabolism of acetate, formate, and ethanol. In addition,
475 pyruvate:ferredoxin oxidoreductase and alcohol dehydrogenase have also been reported to be

476 important fermentation-mediating enzymes in Baltic Sea sediments [105]. Similar to the dynamics
477 of the ABC transporters, the fermentation-mediating enzymes also reflected the overall dynamics of
478 the metabolic profile. Formate dehydrogenase, pyruvate:ferredoxin oxidoreductase, and alcohol
479 dehydrogenase showed increased proportions in the deeper parts of the vegetated compared to the
480 nonvegetated sediment before the decay of roots and rhizomes, reflecting the higher organic matter
481 content and possibly a higher fermentation rate in seagrass-inhabited sediments [11, 15].

482 The final step in the anaerobic degradation of organic matter involves the utilisation of simpler
483 compounds such as SCFAs, including acetate and formate, and alcohols by the sulphate-reducing
484 bacteria or methanogens [8, 9]. One of the most prominent proteins in functional COG category
485 C was adenylylsulphate reductase, which is involved in dissimilatory sulphate reduction (Fig.
486 6). Dissimilatory sulphate reduction is known to be a predominant terminal pathway of organic
487 matter mineralisation in anoxic seabeds [90]. Sulphate adenylyltransferase (Sat), adenylylsulphate
488 reductase (Apr), and dissimilatory sulphite reductase (Dsr), enzymes involved in the dissimilatory
489 sulphate reduction pathway shared by known sulphate-reducing microorganisms [90], were also
490 detected in our metaproteomic dataset. The dynamics of these enzymes showed some common
491 patterns that were comparable to the overall dynamics of the metabolic profile. Overall, higher
492 proportions of these enzymes were found in the deeper parts of the vegetated compared to the
493 nonvegetated site before roots and rhizomes decay, while such differences were not present during
494 decay. This pattern as well as the overall dynamics of the metabolic profile could be explained by
495 the higher organic matter content in the seagrass-inhabited sediments before decay [11, 15] and by
496 the increased input of fresh organic matter into the nonvegetated area during decay, probably as a
497 result of increased resuspension rates and sediment mixing [85].

498 **Conclusions**

499 Metaproteomics has great potential to provide insights into the microbial response to
500 environmental change in marine systems [36]. In the present study, metaproteomic analysis of
501 MS/MS spectra using sequenced metagenomes from a subset of the same samples led to the
502 identification of 57,305 proteins, more than in other metaproteomic studies of marine sediments [38,
503 40–42, 106]. Using this approach, it was possible to assess the dynamics of the metabolic profile
504 of microbial communities in the sediment of a declining *C. nodosa* meadow and the surrounding
505 nonvegetated sediment. Consequently, it was possible to assess the impact of seagrass decline on
506 the metabolic profile of these communities. Seagrass sediments are considered natural hotspots for
507 carbon sequestration, as some estimates suggest that up to 20 % of global carbon sequestration in
508 marine sediments occurs in these carbon-rich sediments, although they occupy only 0.1 % of the
509 seafloor [107–109]. Due to the role of seagrasses in carbon sequestration and their decline observed
510 worldwide [26, 28–34], it is important to gain knowledge about the influence of this phenomenon
511 on the processes carried out by the microbial community in the sediment. The results of the
512 present study show that the differences in the metabolic profile between the microbial communities
513 inhabiting the vegetated and nonvegetated sediment, which were observed in the period before the
514 decay of roots and rhizomes, disappear during decay and lead to similar profiles. Moreover, the
515 metabolic profile of the nonvegetated communities approached that of the vegetated communities
516 during decay. This phenomenon was more pronounced in the deeper parts of the nonvegetated
517 sediment, indicating a stronger influence of decay on the metabolic profile of the communities in
518 this sediment layer.

519 **Declarations**

520 **Ethics approval and consent to participate**

521 Not applicable.

522 **Consent for publication**

523 Not applicable.

524 **Availability of data and material**

525 The raw metagenomic sequences obtained in this study have been deposited in the European
526 Nucleotide Archive (ENA) at EMBL-EBI under the accession number PRJEB75905 (<https://www.ebi.ac.uk/ena/browser/view/PRJEB75905>). The mass spectrometry proteomics data have
527 been deposited in the ProteomeXchange Consortium via the PRIDE [110] partner repository with
528 the dataset identifier PXD054602. Following the recommendations given from the Riffomonas
529 project to enhance data reproducibility (<http://www.riffomonas.org>), the detailed analysis procedure,
530 including the R Markdown file for this article, is available as a GitHub repository (https://github.com/MicrobesRovinj/Markovski_SalineSedimentMetap_EnvironMicrobiome_2025).
531
532

533 **Competing interests**

534 The authors declare that they have no competing interests.

535 **Funding**

536 This study was funded by the Croatian Science Foundation as part of the MICRO-SEAGRASS
537 project (project number IP-2016-06-7118). GJH and ZZ were supported by the Austrian Science
538 Fund (FWF; project number I 4978-B).

539 **Authors' contributions**

540 MN, GJH, and MK designed the study. MM, MN, ZZ, and MK performed sampling and
541 laboratory analyses. MM, ZZ, and MK analysed the data. MM prepared the manuscript with
542 editorial help from MN, ZZ, GJH, and MK. All authors reviewed the manuscript and approved the
543 final submitted version.

544 **Acknowledgements**

545 We thank the Division of Computational Systems Biology (CUBE) of the University of Vienna
546 for access to the Life Science Compute Cluster (LiSC) and Paolo Paliaga for his help with sampling.

547 **References**

- 548 1. Hoshino T, Doi H, Uramoto G-I, Wörmer L, Adhikari RR, Xiao N, et al. Global diversity of
549 microbial communities in marine sediment. Proc Natl Acad Sci U S A. 2020;117:27587–97.
- 550 2. Nealson KH. Sediment bacteria: Who's there, what are they doing, and what's new? Annu Rev
551 Earth Planet Sci. 1997;25:403–34.
- 552 3. Kallmeyer J, Pockalny R, Adhikari RR, Smith DC, D'Hondt S. Global distribution of microbial
553 abundance and biomass in subseafloor sediment. Proc Natl Acad Sci U S A. 2012;109:16213–6.
- 554 4. Petro C, Starnawski P, Schramm A, Kjeldsen K. Microbial community assembly in marine
555 sediments. Aquat Microb Ecol. 2017;79:177–95.
- 556 5. Røy H, Kallmeyer J, Adhikari RR, Pockalny R, Jørgensen BB, D'Hondt S. Aerobic microbial
557 respiration in 86-million-year-old deep-sea red clay. Science. 2012;336:922–5.
- 558 6. Orsi WD. Ecology and evolution of seafloor and subseafloor microbial communities. Nat Rev
559 Microbiol. 2018;16:671–83.
- 560 7. Jørgensen BB. Bacteria and marine biogeochemistry. In: Schulz HD, Zabel M, editors. Marine
561 Geochemistry. Berlin, Heidelberg: Springer; 2000. p. 169–206.
- 562 8. Arndt S, Jørgensen BB, LaRowe DE, Middelburg JJ, Pancost RD, Regnier P. Quantifying
563 the degradation of organic matter in marine sediments: A review and synthesis. Earth-Sci Rev.
564 2013;123:53–86.
- 565 9. Suominen S, van Vliet DM, Sánchez-Andrea I, van der Meer MTJ, Sinninghe Damsté JS,
566 Villanueva L. Organic matter type defines the composition of active microbial communities
567 originating from anoxic Baltic Sea sediments. Front Microbiol. 2021;12:628301.
- 568 10. Arnosti C. Microbial extracellular enzymes and the marine carbon cycle. Annu Rev Mar Sci.
569 2011;3:401–25.
- 570 11. Duarte CM, Holmer M, Marbà N. Plant–microbe interactions in seagrass meadows. In:
571 Kristensenn E, Haese RR, Kostka JE, editors. Interactions Between Macro- and Microorganisms in
572 Marine Sediments. American Geophysical Union (AGU); 2005. p. 31–60.
- 573 12. Peduzzi P, Herndl GJ. Decomposition and significance of seagrass leaf litter (*Cymodocea*

- 574 *nodosa*) for the microbial food web in coastal waters (Gulf of Trieste, Northern Adriatic Sea). Mar
575 Ecol-Prog Ser. 1991;71:163–74.
- 576 13. Liu S, Jiang Z, Deng Y, Wu Y, Zhao C, Zhang J, et al. Effects of seagrass leaf litter decomposition
577 on sediment organic carbon composition and the key transformation processes. Sci China Earth Sci.
578 2017;60:2108–17.
- 579 14. Trevathan-Tackett SM, Jeffries TC, Macreadie PI, Manojlovic B, Ralph P. Long-term
580 decomposition captures key steps in microbial breakdown of seagrass litter. Sci Total Environ.
581 2020;705:135806.
- 582 15. Mohapatra M, Manu S, Dash SP, Rastogi G. Seagrasses and local environment control the
583 bacterial community structure and carbon substrate utilization in brackish sediments. J Environ
584 Manage. 2022;314:115013.
- 585 16. Cúcio C, Engelen AH, Costa R, Muyzer G. Rhizosphere microbiomes of european seagrasses
586 are selected by the plant, but are not species specific. Front Microbiol. 2016;7 MAR, MAR:440.
- 587 17. Zheng P, Wang C, Zhang X, Gong J. Community structure and abundance of *Archaea* in
588 a *Zostera marina* meadow: A comparison between seagrass-colonized and bare sediment sites.
589 Archaea. 2019;2019:5108012.
- 590 18. Alsaffar Z, Pearman JK, Cúrdia J, Ellis J, Calleja ML, Ruiz-Compean P, et al. The role
591 of seagrass vegetation and local environmental conditions in shaping benthic bacterial and
592 macroinvertebrate communities in a tropical coastal lagoon. Sci Rep. 2020;10:13550.
- 593 19. Sun Y, Song Z, Zhang H, Liu P, Hu X. Seagrass vegetation affect the vertical organization of
594 microbial communities in sediment. Mar Environ Res. 2020;162:105174.
- 595 20. Zhang X, Zhao C, Yu S, Jiang Z, Liu S, Wu Y, et al. Rhizosphere microbial community
596 structure is selected by habitat but not plant species in two tropical seagrass beds. Front Microbiol.
597 2020;11:161.
- 598 21. Markovski M, Najdek M, Herndl GJ, Korlević M. Compositional stability of sediment microbial
599 communities during a seagrass meadow decline. Front Mar Sci. 2022;9:966070.
- 600 22. Ettinger CL, Voerman SE, Lang JM, Stachowicz JJ, Eisen JA. Microbial communities in

- 601 sediment from *Zostera marina* patches, but not the *Z. marina* leaf or root microbiomes, vary in
602 relation to distance from patch edge. PeerJ. 2017;5:e3246.
- 603 23. Smith A, Kostka J, Devereux R, Yates D. Seasonal composition and activity of sulfate-reducing
604 prokaryotic communities in seagrass bed sediments. Aquat Microb Ecol. 2004;37:183–95.
- 605 24. Guevara R, Ikenaga M, Dean AL, Pisani C, Boyer JN. Changes in sediment bacterial community
606 in response to long-term nutrient enrichment in a subtropical seagrass-dominated estuary. Microb
607 Ecol. 2014;68:427–40.
- 608 25. Bourque AS, Vega-Thurber R, Fourqurean JW. Microbial community structure and dynamics in
609 restored subtropical seagrass sediments. Aquat Microb Ecol. 2015;74:43–57.
- 610 26. Dunic JC, Brown CJ, Connolly RM, Turschwell MP, Côté IM. Long-term declines and recovery
611 of meadow area across the world's seagrass bioregions. Glob Change Biol. 2021;27:4096–109.
- 612 27. den Hartog C. The Sea-Grasses of the World. Amsterdam, London: North-Holland Publishing
613 Company; 1970.
- 614 28. Tuya F, Martín JA, Luque A. Impact of a marina construction on a seagrass bed at Lanzarote
615 (Canary Islands). J Coast Conserv. 2002;8:157–62.
- 616 29. Orth RJ, Carruthers TJB, Dennison WC, Duarte CM, Fourqurean JW, Heck KL, et al. A global
617 crisis for seagrass ecosystems. BioScience. 2006;56:987–96.
- 618 30. Tuya F, Ribeiro-Leite L, Arto-Cuesta N, Coca J, Haroun R, Espino F. Decadal changes in the
619 structure of *Cymodocea nodosa* seagrass meadows: Natural vs. human influences. Estuar Coast
620 Shelf Sci. 2014;137:41–9.
- 621 31. Fabbri F, Espino F, Herrera R, Moro L, Haroun R, Riera R, et al. Trends of the seagrass
622 *Cymodocea nodosa* (Magnoliophyta) in the Canary Islands: Population changes in the last two
623 decades. Sci Mar. 2015;79:7–13.
- 624 32. Orlando-Bonaca M, Francé J, Mavrič B, Grego M, Lipej L, Flander-Putrel V, et al. A new index
625 (MediSkew) for the assessment of the *Cymodocea nodosa* (Ucria) Ascherson meadow's status. Mar
626 Environ Res. 2015;110:132–41.
- 627 33. Orlando-Bonaca M, Francé J, Mavrič B, Lipej L. Impact of the port of Koper on *Cymodocea*

- 628 *nodososa* meadow. Ann-Anal Istrske Mediteranske. 2019;29:187–94.
- 629 34. Najdek M, Korlević M, Paliaga P, Markovski M, Ivančić I, Iveša L, et al. Dynamics of
630 environmental conditions during the decline of a *Cymodocea nodosa* meadow. Biogeosciences.
631 2020;17:3299–315.
- 632 35. Wilmes P, Heintz-Buschart A, Bond PL. A decade of metaproteomics: Where we stand and
633 what the future holds. Proteomics. 2015;15:3409–17.
- 634 36. Saito MA, Bertrand EM, Duffy ME, Gaylord DA, Held NA, Hervey WJ, et al. Progress and
635 challenges in ocean metaproteomics and proposed best practices for data sharing. J Proteome Res.
636 2019;18:1461–76.
- 637 37. Grossart H-P, Massana R, McMahon KD, Walsh DA. Linking metagenomics to aquatic microbial
638 ecology and biogeochemical cycles. Limnol Oceanogr. 2020;65:S2–20.
- 639 38. Stokke R, Roalkvam I, Lanzen A, Haflidason H, Steen IH. Integrated metagenomic and
640 metaproteomic analyses of an ANME-1-dominated community in marine cold seep sediments.
641 Environ Microbiol. 2012;14:1333–46.
- 642 39. Glass JB, Yu H, Steele JA, Dawson KS, Sun S, Chourey K, et al. Geochemical, metagenomic
643 and metaproteomic insights into trace metal utilization by methane-oxidizing microbial consortia in
644 sulphidic marine sediments. Environ Microbiol. 2014;16:1592–611.
- 645 40. Urich T, Lanzén A, Stokke R, Pedersen RB, Bayer C, Thorseth IH, et al. Microbial community
646 structure and functioning in marine sediments associated with diffuse hydrothermal venting assessed
647 by integrated meta-omics. Environ Microbiol. 2014;16:2699–710.
- 648 41. Lin R, Lin X, Guo T, Wu L, Zhang W, Lin W. Metaproteomic analysis of bacterial communities
649 in marine mudflat aquaculture sediment. World J Microbiol Biotechnol. 2015;31:1397–408.
- 650 42. Bargiela R, Herbst F-A, Martínez-Martínez M, Seifert J, Rojo D, Cappello S, et al.
651 Metaproteomics and metabolomics analyses of chronically petroleum-polluted sites reveal
652 the importance of general anaerobic processes uncoupled with degradation. Proteomics.
653 2015;15:3508–20.
- 654 43. Pjevac P, Meier DV, Markert S, Hentschker C, Schweder T, Becher D, et al. Metaproteogenomic

- 655 profiling of microbial communities colonizing actively venting hydrothermal chimneys. *Front*
656 *Microbiol.* 2018;9:680.
- 657 44. Zhou J, Bruns MA, Tiedje JM. DNA recovery from soils of diverse composition. *Appl Environ*
658 *Microbiol.* 1996;62:316–22.
- 659 45. Li D, Liu C-M, Luo R, Sadakane K, Lam T-W. MEGAHIT: An ultra-fast single-node solution
660 for large and complex metagenomics assembly via succinct de Bruijn graph. *Bioinformatics.*
661 2015;31:1674–6.
- 662 46. Hyatt D, Chen G-L, LoCascio PF, Land ML, Larimer FW, Hauser LJ. Prodigal: Prokaryotic
663 gene recognition and translation initiation site identification. *BMC Bioinformatics.* 2010;11:119.
- 664 47. Cantalapiedra CP, Hernández-Plaza A, Letunic I, Bork P, Huerta-Cepas J. eggNOG-mapper v2:
665 Functional annotation, orthology assignments, and domain prediction at the metagenomic scale.
666 *Mol Biol Evol.* 2021;38:5825–9.
- 667 48. Huerta-Cepas J, Szklarczyk D, Heller D, Hernández-Plaza A, Forslund SK, Cook H, et al.
668 eggNOG 5.0: A hierarchical, functionally and phylogenetically annotated orthology resource based
669 on 5090 organisms and 2502 viruses. *Nucleic Acids Res.* 2019;47:D309–14.
- 670 49. Buchfink B, Reuter K, Drost H-G. Sensitive protein alignments at tree-of-life scale using
671 DIAMOND. *Nat Methods.* 2021;18:366–8.
- 672 50. Chourey K, Jansson J, VerBerkmoes N, Shah M, Chavarria KL, Tom LM, et al. Direct cellular
673 lysis/protein extraction protocol for soil metaproteomics. *J Proteome Res.* 2010;9:6615–22.
- 674 51. Hultman J, Waldrop MP, Mackelprang R, David MM, McFarland J, Blazewicz SJ, et
675 al. Multi-omics of permafrost, active layer and thermokarst bog soil microbiomes. *Nature.*
676 2015;521:208–12.
- 677 52. Wiśniewski JR, Zougman A, Nagaraj N, Mann M. Universal sample preparation method for
678 proteome analysis. *Nat Methods.* 2009;6:359–62.
- 679 53. Korlević M, Markovski M, Zhao Z, Herndl GJ, Najdek M. Selective DNA and protein isolation
680 from marine macrophyte surfaces. *Front Microbiol.* 2021;12:665999.
- 681 54. Ryu S, Gallis B, Goo YA, Shaffer SA, Radulovic D, Goodlett DR. Comparison of a label-free

- 682 quantitative proteomic method based on peptide ion current area to the isotope coded affinity tag
683 method. *Cancer Inform.* 2008;6:243–55.
- 684 55. Zhang Y, Wen Z, Washburn MP, Florens L. Improving label-free quantitative proteomics
685 strategies by distributing shared peptides and stabilizing variance. *Anal Chem.* 2015;87:4749–56.
- 686 56. R Core Team. R: A language and environment for statistical computing. Vienna, Austria: R
687 Foundation for Statistical Computing; 2024.
- 688 57. Wickham H, Averick M, Bryan J, Chang W, McGowan LD, François R, et al. Welcome to the
689 tidyverse. *J Open Source Softw.* 2019;4:1686.
- 690 58. Wickham H. tidyverse: Easily install and load the tidyverse. 2023.
- 691 59. Xie Y. bookdown: Authoring Books and Technical Documents With R Markdown. 2024.
- 692 60. Wilke CO. cowplot: Streamlined plot theme and plot annotations for ggplot2. 2024.
- 693 61. van den Brand T. ggh4x: Hacks for ggplot2. 2024.
- 694 62. FC M, Davis TL, ggplot2 authors. ggpattern: ggplot2 pattern geoms. 2024.
- 695 63. Ahlmann-Eltze C, Patil I. ggsignif: Significance brackets for ggplot2. 2022.
- 696 64. Zhu H. kableExtra: Construct complex table with kable and pipe syntax. 2024.
- 697 65. Xie Y. knitr: A general-purpose package for dynamic report generation in R. 2024.
- 698 66. Neuwirth E. RColorBrewer: ColorBrewer palettes. 2022.
- 699 67. Henry L, Wickham H. rlang: Functions for base types and core R and tidyverse features. 2024.
- 700 68. Allaire J, Xie Y, Dervieux C, McPherson J, Luraschi J, Ushey K, et al. rmarkdown: Dynamic
701 documents for R. 2024.
- 702 69. Sherrill-Mix S. taxonomizr: Functions to work with NCBI accessions and taxonomy. 2023.
- 703 70. Xie Y. tinytex: Helper functions to install and maintain TeX Live, and compile LaTeX documents.
704 2024.
- 705 71. Oksanen J, Simpson GL, Blanchet FG, Kindt R, Legendre P, Minchin PR, et al. vegan:
706 Community ecology package. 2022.
- 707 72. Xie Y. bookdown: Authoring Books and Technical Documents With R Markdown. Boca Raton,
708 Florida: Chapman; Hall/CRC; 2016.

- 709 73. Constantin A-E, Patil I. *ggsignif*: R package for displaying significance brackets for 'ggplot2'.
710 PsyArXiv. 2021. <https://doi.org/10.31234/osf.io/7awm6>.
- 711 74. Xie Y. *Dynamic Documents With R and knitr*. 2nd edition. Boca Raton, Florida: Chapman;
712 Hall/CRC; 2015.
- 713 75. Xie Y. *knitr*: A comprehensive tool for reproducible research in R. In: Stodden V, Leisch F,
714 Peng RD, editors. *Implementing Reproducible Computational Research*. Chapman; Hall/CRC;
715 2014.
- 716 76. Xie Y, Allaire JJ, Grolemund G. *R Markdown: The Definitive Guide*. Boca Raton, Florida:
717 Chapman; Hall/CRC; 2018.
- 718 77. Xie Y, Dervieux C, Riederer E. *R Markdown Cookbook*. Boca Raton, Florida: Chapman;
719 Hall/CRC; 2020.
- 720 78. Xie Y. *TinyTeX*: A lightweight, cross-platform, and easy-to-maintain LaTeX distribution based
721 on TeX Live. *TUGboat*. 2019;40:30–2.
- 722 79. Jost L. Entropy and diversity. *Oikos*. 2006;113:363–75.
- 723 80. Legendre P, Legendre L. *Numerical Ecology*. 3rd edition. Amsterdam: Elsevier; 2012.
- 724 81. Borcard D, Gillet F, Legendre P. *Numerical Ecology With R*. 2nd edition. Springer International
725 Publishing; 2018.
- 726 82. Duarte CM, Chiscano CL. Seagrass biomass and production: A reassessment. *Aquat Bot.*
727 1999;65:159–74.
- 728 83. Duarte CM. Seagrass ecosystems. In: Levin SA, editor. *Encyclopedia of Biodiversity*. 1st
729 edition. Academic Press; 2001. p. 255–68.
- 730 84. Holmer M, Duarte CM, Boschker HTS, Barrón C. Carbon cycling and bacterial carbon sources
731 in pristine and impacted Mediterranean seagrass sediments. *Aquat Microb Ecol*. 2004;36:227–37.
- 732 85. van Katwijk MM, Bos AR, Hermus DCR, Suykerbuyk W. Sediment modification by seagrass
733 beds: Muddification and sandification induced by plant cover and environmental conditions. *Estuar
734 Coast Shelf Sci*. 2010;89:175–81.
- 735 86. Habibi N, Uddin S, Al-Sarawi H, Aldhameer A, Shajan A, Zakir F, et al. Metagenomes from

- 736 coastal sediments of Kuwait: Insights into the microbiome, metabolic functions and resistome.
737 Microorganisms. 2023;11:531.
- 738 87. Kühlbrandt W. Structure and mechanisms of F-type ATP synthases. Annu Rev Biochem.
739 2019;88:515–49.
- 740 88. Baykov AA, Malinen AM, Luoto HH, Lahti R. Pyrophosphate-fueled Na⁺ and H⁺ transport in
741 prokaryotes. Microbiol Mol Biol Rev. 2013;77:267–76.
- 742 89. Luoto HH, Belogurov GA, Baykov AA, Lahti R, Malinen AM. Na⁺-translocating membrane
743 pyrophosphatases are widespread in the microbial world and evolutionarily precede H⁺-translocating
744 pyrophosphatases. J Biol Chem. 2011;286:21633–42.
- 745 90. Jørgensen BB, Findlay AJ, Pellerin A. The biogeochemical sulfur cycle of marine sediments.
746 Front Microbiol. 2019;10:849.
- 747 91. Burdige DJ. Preservation of organic matter in marine sediments: Controls, mechanisms, and an
748 imbalance in sediment organic carbon budgets? Chem Rev. 2007;107:467–85.
- 749 92. Aspeborg H, Coutinho PM, Wang Y, Brumer H, Henrissat B. Evolution, substrate specificity
750 and subfamily classification of glycoside hydrolase family 5 (GH5). BMC Evol Biol. 2012;12:186.
- 751 93. Berlemont R, Martiny AC. Glycoside hydrolases across environmental microbial communities.
752 PLoS Comput Biol. 2016;12:e1005300.
- 753 94. Drula E, Garron M-L, Dogan S, Lombard V, Henrissat B, Terrapon N. The carbohydrate-active
754 enzyme database: Functions and literature. Nucleic Acids Res. 2022;50:D571–7.
- 755 95. Pfeifer L, Classen B. The cell wall of seagrasses: Fascinating, peculiar and a blank canvas for
756 future research. Front Plant Sci. 2020;11:588754.
- 757 96. Torbatinejad N, Sabin J. Laboratory evaluation of some marine plants on South Australian
758 beaches. J Agric Sci Technol. 2001;3:91–100.
- 759 97. Syed NFN, Zakaria MH, Bujang JS. Fiber characteristics and papermaking of seagrass using
760 hand-beaten and blended pulp. BioResources. 2016;11:5358–80.
- 761 98. Zhou M-Y, Wang G-L, Li D, Zhao D-L, Qin Q-L, Chen X-L, et al. Diversity of both the
762 cultivable protease-producing bacteria and bacterial extracellular proteases in the coastal sediments

- 763 of King George Island, Antarctica. PLoS One. 2013;8:e79668.
- 764 99. Zhang X-Y, Han X-X, Chen X-L, Dang H-Y, Xie B-B, Qin Q-L, et al. Diversity of cultivable
765 protease-producing bacteria in sediments of Jiaozhou Bay, China. Front Microbiol. 2015;6:1021.
- 766 100. Liu Z, Liu G, Guo X, Li Y, Ji N, Xu X, et al. Diversity of the protease-producing bacteria
767 and their extracellular protease in the coastal mudflat of Jiaozhou Bay, China: In response to clam
768 naturally growing and aquaculture. Front Microbiol. 2023;14:1164937.
- 769 101. Wang S, Yan Z, Wang P, Zheng X, Fan J. Comparative metagenomics reveals the microbial
770 diversity and metabolic potentials in the sediments and surrounding seawaters of Qinhuangdao
771 mariculture area. PLoS One. 2020;15:e0234128.
- 772 102. Graue J, Engelen B, Cypionka H. Degradation of cyanobacterial biomass in anoxic tidal-flat
773 sediments: A microcosm study of metabolic processes and community changes. ISME J.
774 2012;6:660–9.
- 775 103. Pelikan C, Wasmund K, Glombitza C, Hausmann B, Herbold CW, Flieder M, et al. Anaerobic
776 bacterial degradation of protein and lipid macromolecules in subarctic marine sediment. ISME J.
777 2021;15:833–47.
- 778 104. Zhuang G-C, Lin Y-S, Elvert M, Heuer VB, Hinrichs K-U. Gas chromatographic analysis
779 of methanol and ethanol in marine sediment pore waters: Validation and implementation of three
780 pretreatment techniques. Mar Chem. 2014;160:82–90.
- 781 105. Zinke LA, Glombitza C, Bird JT, Røy H, Jørgensen BB, Lloyd KG, et al. Microbial organic
782 matter degradation potential in Baltic Sea sediments is influenced by depositional conditions and *in*
783 *situ* geochemistry. Appl Environ Microbiol. 2019;85:e02164–18.
- 784 106. Gillan DC, Roosa S, Kunath B, Billon G, Wattiez R. The long-term adaptation of bacterial
785 communities in metal-contaminated sediments: A metaproteogenomic study. Environ Microbiol.
786 2015;17:1991–2005.
- 787 107. Duarte CM, Kennedy H, Marbà N, Hendriks I. Assessing the capacity of seagrass meadows for
788 carbon burial: Current limitations and future strategies. Ocean Coastal Manage. 2013;83:32–8.
- 789 108. Duarte CM, Middelburg JJ, Caraco N. Major role of marine vegetation on the oceanic carbon

- 790 cycle. *Biogeosciences*. 2005;2:1–8.
- 791 109. Kennedy H, Beggins J, Duarte CM, Fourqurean JW, Holmer M, Marbà N, et al. Seagrass
792 sediments as a global carbon sink: Isotopic constraints. *Glob Biogeochem Cycles*. 2010;24:GB4026.
- 793 110. Perez-Riverol Y, Bai J, Bandla C, García-Seisdedos D, Hewapathirana S, Kamatchinathan
794 S, et al. The PRIDE database resources in 2022: A hub for mass spectrometry-based proteomics
795 evidences. *Nucleic Acids Res*. 2022;50:D543–52.